1356 *Macromolecules* **2010**, *43*, 1356–1363
DOI: 10.1021/ma902399m

Macromolecules
ARTICLE

Morphology of Three-Phase PS/PBA Composite Latex Particles Containing in Situ Produced Block Copolymers

Virginia Herrera,[†,§] Zita Palmillas,[†] Rosangela Pirri,[‡] Yuri Reyes,[†] Jose R. Leiza,[†] and José M. Asua*[,†]

[†]*Institute for Polymer Materials, POLYMAT and Grupo de Ingeniería Química, Departamento de Química Aplicada, Facultad de Ciencias Químicas; University of the Basque Country, Joxe Mari Korta zentroa, Tolosa etorbidea 72, Donostia-San Sebastián 20018, Spain and* [‡]*Arkema, Groupement de Recherches de Lacq, R.N. 117, B.P. 34, F-64170 Lacq, France.* [§]*Current address: Ipagsa Industrial SL, Sant Jordi, 15-Apdo. Correos, 262, 08191 Rubí, Spain.*

Received October 29, 2009; Revised Manuscript Received December 23, 2009

ABSTRACT: Three-phase styrene−butyl acrylate composite polymer particles were synthesized by combining free radical polymerization, which yielded PS and PBA-*co*-PS, and controlled free radical polymerization, which yielded a large amount of PS-*block*-(PBA-*co*-PS)). Particle morphology evolves from core−shell when the particles did not contain block copolymer to hemispherical when a large amount of block copolymers was produced. The existing models could not predict this change in morphology. A general approach for the calculation of the equilibrium morphology of multiphase particles was developed using a Monte Carlo method.

Introduction

The production of composite latex particles with defined morphology is a problem of great interest as they have a spectrum of application properties broader than particles having uniform composition, and hence they play an important role in coatings, adhesives, impact modifiers, and many other specialty materials.[1,2] Composite latex particles are commonly prepared by seeded emulsion polymerization. The composition of the seed (polymer 1) is different from that of the polymer produced during the polymerization (polymer 2). Polymerization of monomer 2 leads to the formation of chains of polymer 2 in a matrix of polymer 1 swollen with monomer 2. Because of the incompatibility between the two polymers, phase separation occurs and clusters of polymer 2 are formed within the matrix of polymer 1. Polymerization continues in both clusters and matrix, and hence the clusters grow in size and new clusters are formed. In addition, van der Waals forces cause cluster migration toward the equilibrium morphology.[3−5] Depending on the polymerization conditions, a wide variety of particle morphologies can be produced: core−shell,[6] inverted core−shell,[7] hemispheres,[8] raspberry-like,[9] and void particles.[10]

Particle morphology depends on the interplay between thermodynamics and kinetics.[1−5,11,12] Thermodynamics determines the particle morphology at equilibrium, according to the minimum surface free energy. Kinetic factors control whether the particle reaches the equilibrium morphology or remains at a metastable (kinetically stable) morphology. The polymer−polymer and polymer−aqueous phase interfacial tensions play a key role in the development of the particle morphology as they determine the surface free energy. In addition, they strongly affect the kinetics. The driving forces for cluster migration toward the equilibrium morphology are the van der Waals forces among clusters and between clusters and aqueous phase. These forces are related to the interfacial tensions.[3] The lower the interfacial tensions, the lower the van der Waals forces and hence the slower the evolution of the morphology toward equilibrium. Polymer−aqueous phase interfacial tensions are affected by the hydrophilicity of the polymers,[13] the initiator end groups,[14] the type and amount of surfactant,[15,16] and the presence of functional monomers.[13] The polymer−polymer interfacial tension is more difficult to modify. Rajatapiti et al.[17] used graft copolymers to lower this interfacial tension. The authors showed that morphology was severely affected by the presence of the graft copolymer.

The morphology of composite polystyrene (PS)/poly(methyl methacrylate) (PMMA) particles can also be modified by means of block copolymers produced in situ by controlled radical polymerization, allowing the synthesis of particles that could not be produced otherwise.[18,19] These works are a proof of concept for the feasibility of particle morphology modification by in situ synthesis of block copolymers. However, the application of this concept for the synthesis of useful materials is hindered by several reasons. In the previous works, high glass transition temperature (T_g) polymers were used whereas most commercial latexes are low-T_g film forming polymers. Because the cluster migration severely decreases as the T_g of the polymer increases, the effect of the in situ produced block copolymer on the particle morphology observed for the high-T_g polymers cannot be directly extrapolated to low-T_g commercial polymers. Extrapolation would be possible if a theoretical model for the prediction of the equilibrium morphology or the kinetics of the development of the morphology of these types of particles were available. However, the existing kinetic models[3−5] were developed for two-phase systems, whereas these are three-phase particles, because a significant amount of block copolymer was produced. The equilibrium models were also mainly developed for two-phase composite polymer particles. The equilibrium morphology was the one that gives the minimum interfacial energy calculated as the product of the interfacial areas and the interfacial tensions. This requires defining the equilibrium morphology a priori. For two-phase systems, the number of equilibrium morphologies is modest (see Figure 2), but for three-phase

*To whom correspondence should be addressed. E-mail: jm.asau@ehu.es.

 Published on Web 01/14/2010

Table 1. Experimental Details for the Synthesis of Composite PS/PBA Latexes[a]

latex	step 1	step 2		polymer formed in step 2	rel interfacial tensions[b,c]
1	batch miniemulsion polymerization of S without using SG1 (90 °C); $X_S = 0.96$	swelling the S latex (≈150 g) with BA (≈5 g)	addition of AIBN (≈0.12 g) and BA (5 g) and let it polymerize at 90 °C; $X_g = 0.95$	almost pure PBA	σ_{12} = medium; σ_{13} = highest; σ_{23} = high
2	batch miniemulsion polymerization of S in the presence of SG1 (90 °C); $R = 0.45$, $X_S = 0.95$	swelling the S latex (≈150 g) with BA (≈5 g)	addition of AIBN (≈0.12 g) and BA (5 g) and let it polymerize at 90 °C; $X_g = 0.92$	almost pure PBA and PS-*block*-PBA	σ_{12} = low; σ_{13} = highest; σ_{23} = high
3	batch miniemulsion polymerization of S in the presence of SG1 (90 °C); $R = 0.78$, $X_S = 0.9$	swelling the S latex (≈150 g) with BA (≈5 g)	addition of AIBN (≈0.0040 g) and BA (5 g) and let it polymerize at 90 °C; $X_g = 0.91$	PBA-*co*-PS and PS-*block*-(PBA-*co*-PS)	σ_{12} = low−lowest; σ_{13} = highest; σ_{23} = higher−high
4	batch miniemulsion polymerization of S in the presence of SG1 (90 °C); $R = 1.5$, $X_S = 0.7$	swelling the S latex (≈150 g) with BA (≈5 g)	addition of AIBN (≈0.12) and BA (5 g) and let it polymerize at 90 °C; $X_g = 0.92$	PBA-*co*-PS and PS-*block*-(PBA-*co*-PS)	σ_{12} = lowest; σ_{13} = highest; σ_{23} = higher

[a] X_S: styrene conversion; X_g: final overall conversion of both monomers in step two. R = [SG1]/[AIBN]. The amount of BA added in the second step was adjusted to yield latexes with S/BA = 50/50 (w/w) composition.The overall conversion in step 2 (X_g) was measured after 24 h of polymerization. [b] The values of interfacial tensions are all on a relative scale: highest (σ_{13}) → higher → high → medium → low → lowest (σ_{12} with block copolymers). [c] 1 = styrene; 2 = BA, and 3 = water.

systems the number of possible morphologies tremendously increases. This problem is illustrated in the work of Sundberg and Sundberg,[22] who in order to determine the equilibrium morphology of three-phase systems needed to simplify the geometry of some of the 22 possible morphologies identified to be able to calculate the interfacial area. Another drawback of this method is that it cannot be applied for systems with four or more phases.

This work investigates the effect of the block copolymer produced in situ on the particle morphology of styrene−butyl acrylate film forming latexes. Polymerizations were carried out under a variety of conditions including those in which a high amount of PS-*block*-PBA copolymers were obtained. This led to particle morphology that could not be accounted for by the straightforward application of the existing models for either equilibrium morphology or kinetics of particle morphology development. Modification of the existing models and a newly developed model were used to analyze the particle morphologies observed.

Polymerization Strategy

The polymerization strategy includes the following steps:

1. *Seed Preparation*: The seed was synthesized by miniemulsion polymerization of styrene. A certain amount of controlled radical polymerization agent was added at the beginning of the polymerization. Although there are no limitations with respect to the type of controlled radical polymerization agent used (nitroxides, RAFT and ATRP agents can be used provided that a polyBA block can be produced in the second stage), in this work a nitroxide (*N*-*tert*-butyl-*N*-(1-diethylphosphono-2,2-dimethylpropyl), SG1) was used. The amount of PS chains capped by the nitroxide depended on the amount of SG1 used during the preparation of the seed. The higher the amount of SG1 used, the higher the number of PS chains capped with SG1 and hence able to grow in the second step with BA. Consequently, the larger the number of block copolymer chains in the composite particle.

2. *Composite Latex*: BA was added together with additional initiator. When the poly(S)−SG1 dormant chains dissociate into active polymer chains and nitroxide radicals, the polymer chain would react with BA, yielding a block copolymer. The final polymer particle was composed of polystyrene, poly(S-*block*-BA), and poly(butyl acrylate) if styrene completely reacted during the synthesis of the seed and of polystyrene, poly(S-*block*-(BA-*co*-S)), and poly(BA-*co*-S) if unreacted styrene remained when BA was added.

Table 2. Formulation Used To Prepare the PS Seeds of the First Stage[a]

ingredients	amount (g)
styrene	39.5
AIBN	0.28
SDS	1.5
$NaHCO_3$	0.28
hexadecane	2.4
polystyrene	0.31

[a] R = [SG1]/[AIBN]. Solids content = 11 wt %. $R_{latex\,1} = 0$; $R_{latex\,2} = 0.45$; $R_{latex\,3} = 0.78$; $R_{latex\,4} = 1.5$.

Experimental Part

Materials. Styrene and *n*-butyl acrylate monomers (Quimidroga) were washed with a 10 wt % aqueous solution of sodium hydroxide to remove the inhibitor before use. After that, calcium chloride anhydrous ($CaCl_2$) was added to remove all remaining water, and then the monomers were stored in a refrigerator until use. The initiator, azobis(isobutyronitrile) (AIBN, Aldrich); the polystyrene (M_w = 280 000, Aldrich); the buffer, sodium hydrogen carbonate ($NaHCO_3$, Aldrich); the surfactant, sodium dodecyl sulfate (SDS, Aldrich); and the costabilizer, hexadecane (Aldrich), were used as received. The controlled radical polymerization agent, *N*-*tert*-butyl-*N*-(1-diethylphosphono-2,2-dimethylpropyl) nitroxide (SG1, kindly supplied by Arkema), was used as received.

Latex Preparation. Table 1 summarizes the PS/PBA composite latexes (latexes 1−4) prepared in this work. All the latexes had the same overall composition (50/50 wt/wt) and were prepared under the same conditions, but using different amounts of SG1 during the preparation of the polystyrene seed (first step). Table 2 shows the formulation used in the preparation of the seeds by miniemulsion polymerization in a batch reactor, under a nitrogen atmosphere at 90 °C and using AIBN as initiator. Hexadecane was used as cosurfactant (to stabilize the droplets from Ostwald ripening), and its effect was enhanced with a high molar mass polystyrene.[23] The organic phase made by dissolving SG1, the hexadecane, and the polystyrene in the monomer was added to an aqueous solution containing

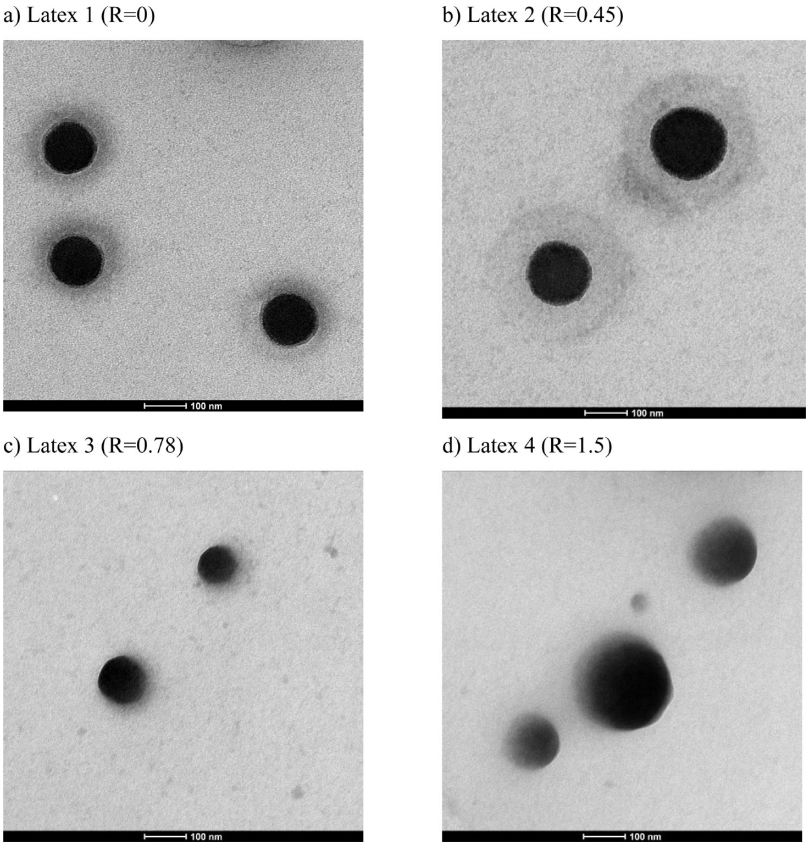

Figure 1. Morphology of composite particles of PS/PBA synthesized with the formulation of Table 1.

the buffer and the surfactant. The solutions were sonicated for 10 min in a Branson 450 Sonifier (power 7, duty cycle: 60%) under magnetic stirring. Latex 1 was prepared without SG1 (R = [SG1]/[AIBN] = 0), and it was used as a reference. Latexes 2−4 contained increasing amounts of SG1 in the seed.

In the second step, the seeds (150 g) were swollen with BA (5 g) at room temperature and under magnetic stirring overnight. The swollen latex was heated to 90 °C and maintained for 4 h before the addition of more BA (5 g) and AIBN (0.12 g). The total amount of BA added was adjusted to yield a PS/PBA overall copolymer composition of 50/50 (w/w) at full conversion. The resulting mixtures were polymerized at 90 °C (see Table 1 for additional details). In the preparation of the seeds, the styrene conversion (X_S in Table 1) was not complete. Therefore, in the second stage, a BA-rich p(S-*co*-BA) copolymer was produced. The higher the conversion in the first stage, the lower the amount of S in the copolymer. Note that X_g in Table 1 refers to the overall conversion based on both monomers in the second step. As the amount of SG1 used in each seed was different, the amount of block copolymers formed in the second step was different, too. This allowed studying the effect of different amounts of block copolymers on the PS/PBA particle morphology.

Latex Characterization. Monomer conversion was determined by gravimetry. Molar mass distributions were measured by size exclusion chromatography (SEC). SEC was performed using a Waters apparatus equipped with a Waters model 510 pump, three Styragel columns in series (HR 2, HR 4, HR 6), and two detectors (Waters 2410 RI detector and Waters 2487 UV detector), at 35 °C with tetrahydrofuran (THF) as eluent. At a wavelength of 262 nm, absorption by poly(butyl acrylate) is minimal, and hence it was considered as "invisible". Therefore, the formation of PS chains and the growth of the nitroxide-capped polystyrene chains during the second step can be tracked by using the UV detector on the SEC at λ = 262 nm.

The morphology of latex particles was studied by transmission electron microscopy, TEM (Hitachi 7000 at 75 kV). The images were taken at ×80 000 magnification. The original latexes were diluted with a 0.5% aqueous solution of phosphotungstic acid (PTA) stain. A drop of each dilute latex was placed on a carbon-coated Formvar film deposited on a copper grid and dried with an UV lamp. Then, the samples were stained with ruthenium tetroxide (RuO_4) vapor for 1 h. This allows to differentiate between PS and PBA domains in the micrographs (PS appears dark whereas PBA appears clear).

Liquid adsorption chromatography (LAC) was performed using a high-performance liquid chromatograph where the mobile phase used was a mixture of THF and hexane. Under these conditions, PBA chains eluted before PS chains and the block copolymers of PS/PBA eluted between the pure polymers. Homopolymer standards were used as reference.

Results and Discussion

Morphology of the Latexes. Figure 1 presents the TEM pictures of the final latex for the four experiments described in Table 1, which were prepared with different amounts of SG1 in the first step of the polymerization. It can be seen that in polymerizations carried out in absence of SG1 (latex 1) or with small amounts of SG1 (latex 2, R = 0.45) core−shell morphologies were observed, with the PS in the core and the PBA in the shell. Note that the size of the shell was larger than that expected from the amount of BA added in the second stage. This was due to the low T_g of the PBA shell and to the TEM sample analysis procedure. The samples were analyzed at room temperature, and the soft shell might spread over. The thicker shell of latex 2 in comparison to latex 1 was due to its larger particle size ($dp_{latex\,1}$ = 170 nm; $dp_{latex\,2}$ = 255 nm, measured by dynamic light scattering). For the experiments carried out with higher amounts of SG1

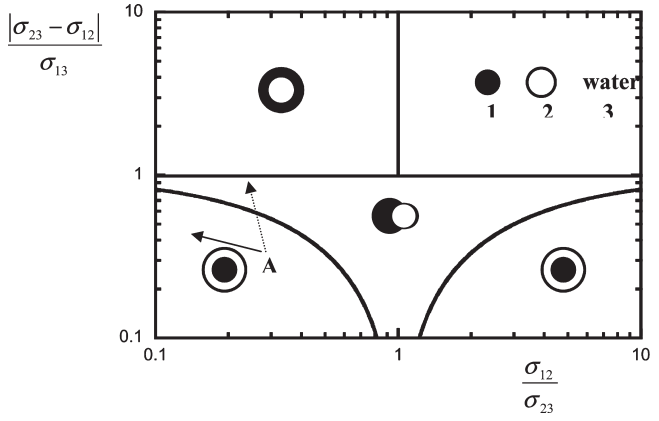

Figure 2. Equilibrium morphologies: ●, polymer 1 (seed); ○, polymer 2 (produced by polymerization of the second step monomer). Subscript indexes in the interfacial tensions (1, 2, and 3) refer to polymer 1 (PS), polymer 2 (PBA and/or PBA-*co*-PS), and water, respectively.

(latex 3 and mainly latex 4), hemispherical morphologies were obtained. The change in morphology was likely due to the higher fraction of block copolymer that reduced the interfacial tension between PS and PBA-*co*-PS. In an attempt to confirm this hypothesis, the morphologies were analyzed using the equilibrium morphology map[3] presented in Figure 2. This map was developed by calculating the morphologies that provided the minimum surface energy for a two-phase composite particle. Depending on the values of the interfacial tensions, the equilibrium morphology can be core−shell (left and right bottom corners), inverted core−shell (left upper quadrant), hemispherical, and separated particles (right upper quadrant). The values of the interfacial tensions PS/water (σ_{13}), polymer/polymer (σ_{12}), and PBA-*co*-PS/water (σ_{23}) are needed in order to estimate the equilibrium morphologies. The exact values of these interfacial tensions were not available, but valuable information could be obtained from relative values. The interfacial tension PS/water (σ_{13}) was larger than the PBA-*co*-PS/water (σ_{23}) because PS is more hydrophobic than PBA. In addition, for latex 1 the polymer−polymer interfacial tension (σ_{12}) would be significant (there was no block copolymer in this latex) but smaller than σ_{23}. These led to $\sigma_{12}/\sigma_{23} < 1$ and $|\sigma_{23} - \sigma_{12}|/\sigma_{13} < 1$ and hence to core−shell morphology (exemplified by point A in Figure 2), which agrees with the morphology of latex 1 (Figure 1a). The main effect of the presence of block copolymer was to reduce σ_{12}. For latex 2 the values of σ_{13} and σ_{23} should be similar to those of latex 1. Simple calculations show that the decrease of σ_{12} cannot shift the position of point A outside of the region of core−shell morphology (Supporting Information). This is consistent with the morphology observed for latex 2.

For latex 3, σ_{12} was likely lower than for latex 2 because a higher concentration of SG1 was used (which led to a higher fraction of block copolymers). In addition, σ_{23} should be slightly higher than for latex 2 because of the higher amount of styrene contained in the second stage copolymer. However, these changes are not enough to shift the position of point A outside the region of core−shell morphology (Supporting Information); namely a core−shell morphology was predicted. This is in conflict with the observed morphology (Figure 1c). Similar conflict appeared when latex 4 was analyzed.

Figure 2 deals with equilibrium morphologies, but the change in the interfacial tensions also affects the kinetics of the particle morphology development.[3−5] The lower the interfacial tensions, the lower the van der Waals forces and hence the slower the evolution of the morphology toward the equilibrium. Therefore, the decrease of the polymer−polymer interfacial tension may lead to a kinetically controlled morphology. However, simulations carried out (not shown) using the dynamic model for the development of particle morphology[3−5] did not lead to morphologies similar to those in the Figure 1c,d. This means that some characteristic feature of latexes 3 and 4 was not considered in the kinetic and thermodynamic models.

Figure 3 presents the molar mass distributions for latexes 1−4. The GPC traces were obtained with the two detectors, and for the sake of brevity only the data obtained with the UV detector are shown. Note that the UV detector is only sensitive to the polymer chains containing styrene units. The GPC traces show that only for latexes 3 and 4 the PS chains formed in the first step did grow in size in the second step. The effect was modest for latex 3 but very strong for latex 4 which was synthesized with the highest concentration of SG1, and hence it contained plenty of nitroxide-capped PS chains produced in the first step. Simulations carried out in Predici[24] for the polymerization of styrene in the presence of SG1 predicted that 73% of PS chains were capped with SG1 at the end of the seed preparation for latex 3 and 98% for latex 4. For latex 4 the prediction is consistent with the results presented in Figure 3, but for latex 3, the prediction seems to overestimate the fraction of chains that can undergo chain extension.

Figures 4−6 present the LAC chromatograms for latexes 2−4, respectively. Under the conditions used, the PBA eluted first and the PS later. The block copolymers (if present) should elute between the pure PBA and PS phases. Figure 4 shows that for latex 2 the final latex (in red) was composed by pure PS and PBA phases with no noticeable signal of block copolymer (no peaks were observed between the PBA and PS standards). This in agreement with the GPC results shown in Figure 3b which indicated that the PS chains produced in the first step did not grow noticeably during the second stage polymerization with BA.

Figure 5 shows that with a higher amount of SG1 (R = 0.78) some PBA−PS copolymer chains were produced during the second stage. (The PBA peak was now much broader than that displayed in Figure 4 where no block copolymers were present.) However, this is not a proof that block copolymers were formed because the presence of some random copolymers PBA-*co*-PS could also be produced due to the 10 wt % of free styrene left from the first step (see Table 1). The final latex showed a clear PS peak, which was very similar to the peak of the polymer at the end of step 1. This result agrees with the molar mass distribution of the polymers containing styrene presented in Figure 3c.

Figure 6 presents the LAC chromatogram of latex 4. It can be seen that there was no polymer in the region of pure PBA and that the relative amount of polymer in the region of pure PS was small. Most of the polymer was a PBA−PS copolymer. The shift of the SEC trace in Figure 3c suggests that a large part of this copolymer was a block copolymer, but the presence of random PBA-*co*-PS cannot be discharged.

The results available indicate that latexes 3 and 4 contained three types of polymer: PS, PS-*block*-(PBA-*co*-PS), and PBA-*co*-PS. In addition, the amount of block copolymer may be substantial (mainly in the case of latex 4).

Predicting the Morphology of Three-Phase Systems. The models available to predict both the equilibrium morphologies and the dynamics of the morphology[2−5,11,12,20,21] change were mainly developed for two-phase composite polymer particles. Attempts to calculate the equilibrium morphology

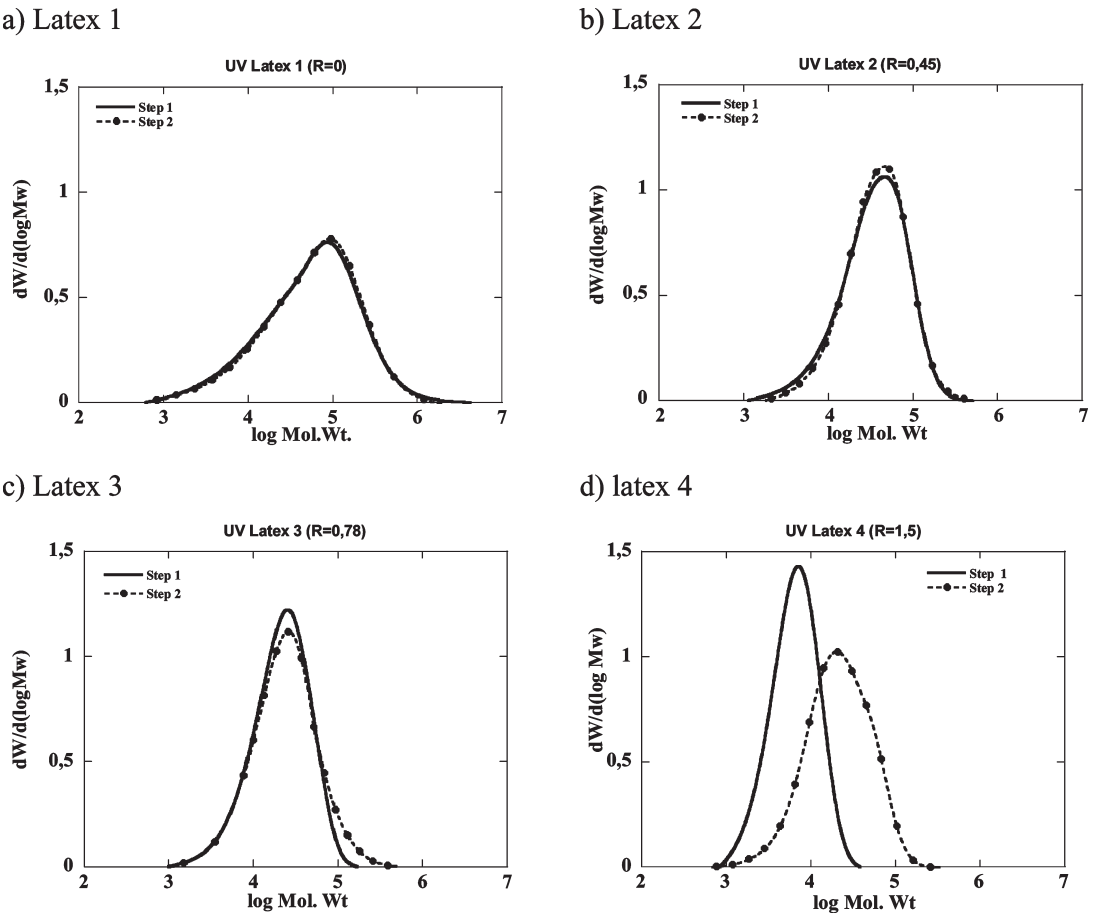

Figure 3. Molar mass distribution experiments of latexes 1−4 using the UV detector at 262 nm.

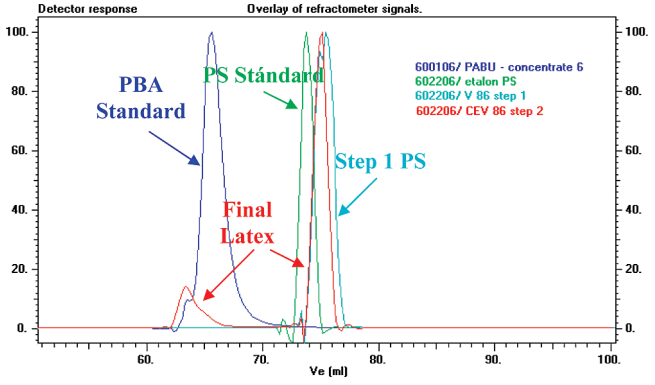

Figure 4. LAC chromatogram for latex 2 (R = 0.45).

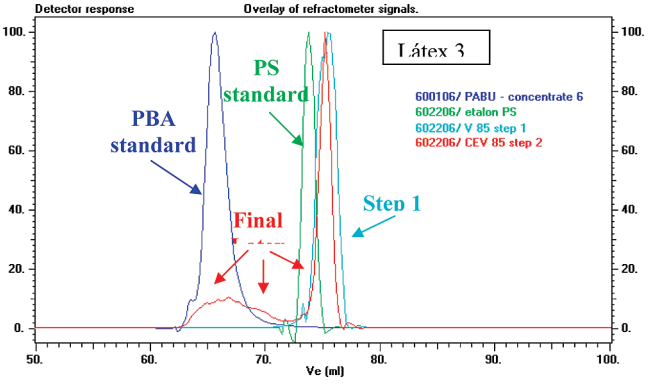

Figure 5. LAC chromatogram for latex 3 (R = 0.78).

of three-phase systems using simplified geometries have been reported.[22]

In this work, two approaches were used to predict the morphology of these three-phase particles. The first one was a shortcut based on the dynamic model by Gonzalez-Ortiz and Asua.[3−5] Because Figures 3d and 6 showed that for latex 4 most polymer chains were copolymers containing both styrene and butyl acrylate, the final polymer was arbitrarily divided in two phases: one rich in styrene and the other rich in butyl acrylate. The interfacial tension between the styrene-rich copolymer and the water should be somewhat higher than that of the butyl acrylate-rich copolymer with water. On the other hand, the polymer/polymer interfacial tension should be very low because of the similar composition of the two phases. In the simulation, it was assumed that polymer 1 had the same interfacial tension as the styrene-rich copolymer and polymer 2 had the same interfacial tension as the butyl acrylate-rich copolymer. Because a not charged initiator was used, a homogeneous distribution of radicals in the particles was considered in the simulations, namely that there were no radical concentration profiles due to the anchoring of the ionic part of the entering radicals to the particle surface.[25,26] Figure 7 shows the time evolution of the simulated morphology. It can be seen that the model predicts that a hemispherical morphology was obtained at the end of the process. The equilibrium morphology was reached because of the low molar mass of the seed polymer (Figure 3d) and the high concentration of monomer in the polymer particle (batch polymerization). Even though the predictions of the model agreed with the experimental

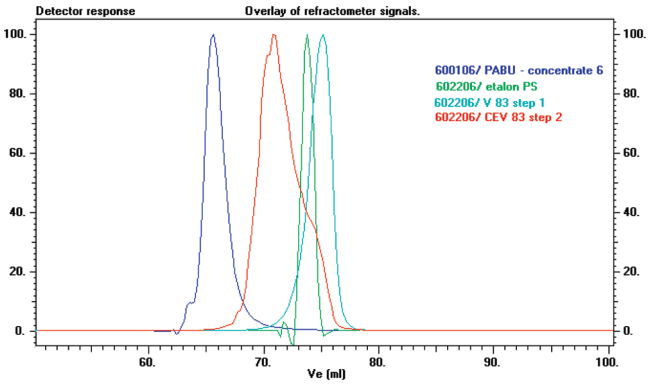

Figure 6. LAC chromatogram for latex 4 ($R = 1.5$).

findings, admittedly, the application of this shortcut is limited, and a more general approach should be developed.

An important piece of information provided by the dynamic model is that the equilibrium morphology was reached. Therefore, in order to analyze the results presented in this work, it would be sufficient to predict the equilibrium morphology of a three-phase polymer particle.

Although the construction of equilibrium morphology maps equivalent to that developed for a two-phase systems (Figure 2) may be possible, the presence of a third phase would tremendously complicate the task. Therefore, a standard canonical Monte Carlo simulation was used[29] to determine the latex particle morphology of a three-phase system. The polymer (PS, PS-*block*-(PS-*co*-PBA), PS-*co*-PBA) and aqueous (W) phases were modeled as hard spheres of unit diameter (which is the unity of length) contained in a spherical simulation cell with "impenetrable walls", i.e., no boundary conditions. The cross-interaction diameter between phases of different components is given by the nonadditive hard sphere potential[30] as follows:

$$U_{ij}(r) = \begin{cases} \infty & \text{if } r \le d_{ij} \\ 0 & \text{if } r > d_{ij} \end{cases} \qquad (1)$$

$$j \neq j$$

where $d_{ij} = 0.5(d_i + d_j)(1 + \Delta_{ij})$ and d_i and d_j are the diameters of the rigid spheres of any of the components. This simple model for the potential was chosen because of its computational efficiency. The nonadditive parameter of this potential, Δ_{ij}, accounts for the incompatibility between different polymers. For spheres made of the same polymer, $\Delta_{ii} = 0$. For different polymers, Δ_{ij} is directly proportional to the interfacial tension between the phases i and j; therefore, the greater the interfacial tension between the components i and j the larger Δ_{ij}.[31] Since the block copolymer shares the properties of both the polystyrene and the PS-*co*-PBA, the nonadditive parameter of this component with respect to water was estimated to be the average of those of these polymers with water. On the other hand, to account for the preferential contact of the polystyrene and the random copolymer with their similar parts of the block copolymer, the nonadditive parameters of the block copolymer with polystyrene and with the random copolymer were taken as half of that of polystyrene with the random copolymer (see caption of Figure 8).

Initially, no less than 7000 spheres (half of them considered as water) were randomly inserted in a spherical simulation cell with a nominal diameter equal to 30. Water spheres are allowed to get closer to the simulation cell walls, while all other components cannot, to mimic a continuous aqueous

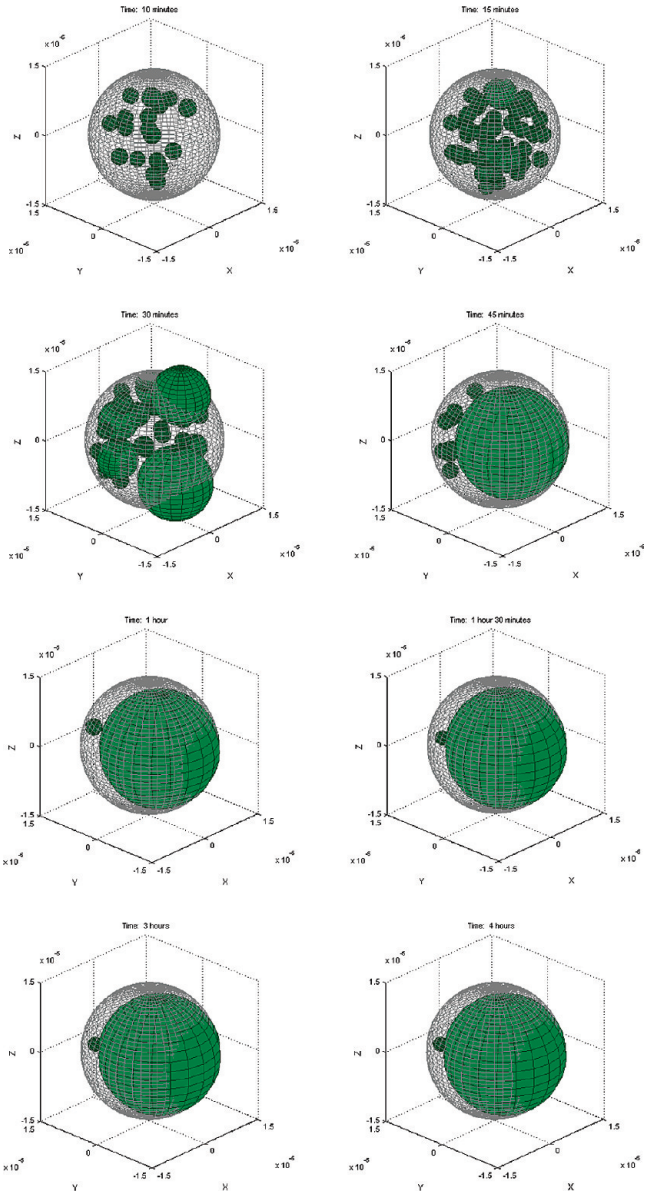

Figure 7. Simulated evolution of the particle morphology of latex 4. Interfacial tensions adapted from refs 27 and 28: $\sigma_{12} = 0.5$ mN/m, $\sigma_{13} = 4.9$ mN/m, and $\sigma_{23} = 4.6$ mN/m.

phase. The system was left to equilibrate for 7×10^6 configurations according to the Metropolis algorithm[29] with an acceptance ratio of 45%.

Figure 8a shows the equilibrium morphology of a particle composed by a 10% of PS, 35% of PS-*co*-PBA, and 55% of PS-*block*-(PS-*co*-PBA) that mimics the polymer achieved in latex 4 (see the Supporting Information for the estimation of the composition of latex 4). Figure 8b is the same morphology in which the block copolymer was made "transparent" to have a clearer view of the PS phase. The nonadditive parameter between the different phases used in the simulation is shown in the figure caption. The simulation predicted a hemispherical-like morphology with the block copolymer phase (dark gray) forming a separate phase between the PS (black) and the PBA-*co*-PS (light gray) . In order to compare the simulated morphology with the TEM picture in Figure 1, the TEM picture of the particle presented in Figure 8a was simulated. It was assumed that the particle received a vertical electron beam and that the detector was a horizontal plane located below the particle. For each point of this plane the

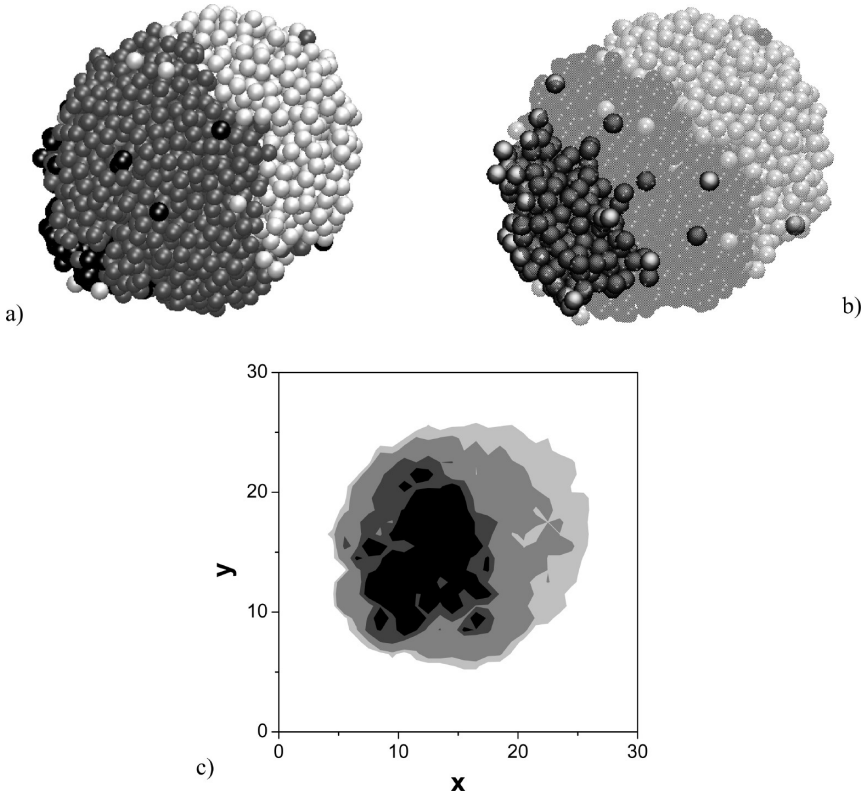

Figure 8. Monte Carlo simulation of the equilibrium morphology of a three-phase system composed by PS, PS-*block*-(PBA-*co*-PS), and PBA-*co*-PS phases. (a) 3-D snapshot; (b)3-D snapshot in which the the block copolymer was made more transparent and (c) TEM simulation. The nonadditive parameters used in the simulation are $\Delta_{\text{PS-PS-}rand\text{-PBA}} = 0.50$; $\Delta_{\text{PS-W}} = 0.75$; $\Delta_{\text{PS-}rand\text{-PBA-W}} = 0.70$. The others were computed as $\Delta_{\text{PS-}block\text{-PBA-W}} = 0.5(\Delta_{\text{PS-W}} + \Delta_{\text{PS-}rand\text{-PBA-W}})$; $\Delta_{\text{PS-}block-\text{PBA-PS}} = 0.5(\Delta_{\text{PS-PS-}rand\text{-PBA}})$; $\Delta_{\text{PS-}block-\text{PBA-PS-}ran\text{-PBA)}} = 0.5(\Delta_{\text{PS-PS-}rand\text{-PBA}})$.

absorption of the electrons was calculated as

$$\text{electron absorption} = \sum_i h_i k_i \qquad (2)$$

where k_i is the absorption coefficient characteristic of polymer i and h_i is the number of spheres of each type that are above each point of the detector plane. The values of the absorption coefficients are unknown, but for the purpose of this simulation, the relative values were sufficient. The absorption coefficients should be ranged as $k_{\text{PS}} > k_{\text{PS-}block\text{-(PS-}co\text{-PBA)}} > k_{\text{PS-}co\text{-PBA}}$ as polystyrene is almost opaque and poly(butyl acrylate) is almost transparent. The values used are $k_{\text{PS}} = 5$, $k_{\text{PS-}block\text{-(PS-}co\text{-PBA)}} = 3.5$, and $k_{\text{PS-}co\text{-PBA}} = 1$. The projection of the electron absorptions on the detector plane is presented in Figure 8c were the darker zones corresponded to the higher absorption. It can be seen that the prediction is in good agreement with the experimental results.

Conclusions

In the foregoing the effect of the in situ produced block copolymer on the particle morphology of styrene−butyl acrylate film forming latexes was investigated. It was found that the morphology evolves from core−shell (PS in the core) morphology, for particles with no or a small amount of block copolymer, to a hemispherical morphology when a large amount of block copolymer was produced. The models available for the prediction of equilibrium morphology accounted for the core−shell morphologies but did not predict the observed hemispherical morphologies. The existing model for the dynamics of the morphology change was used to simulate the evolution of a particle in which the three phases were somehow arbitrarily divided in two phases: one rich in styrene and the other rich in butyl acrylate. Although the morphology predicted by the model agreed well with the observed morphology, the usefulness of this approach is limited. Nevertheless, this model provided important information: the final morphology was an equilibrium morphology.

A general approach for the calculation of the multiphase particle equilibrium morphology based on a Monte Carlo method was developed. The predictions of this model agreed well with the experimental observations. This opens the possibility of using this model to simulate the morphology of multiphase systems, such as polymer−polymer and polymer−inorganic hybrids.

Acknowledgment. The financial support from the Diputacion Foral de Gipuzkoa, Gobierno Vasco (GV 07/16-IT-303-07) and Ministerio de Ciencia y Tecnologia (CTQ 2006-03412 and Programa Consolider-Ingenio 2010 "CIC nanoGUNE Consolider" contract CSD2006-00053) is gratefully acknowledged. The SGI/IZO-SGIker UPV/EHU (supported by the "National Program for the Promotion of Human Resources within the National Plan of Scientific Research, Development and Innovation−Fondo Social Europeo, Gobierno Vasco and MCyT) is gratefully acknowledged for generous allocation of computational resources.

Supporting Information Available: Change in the position of point A in Figure 2 upon variation of the polymer−polymer interfacial tension and estimation of the composition of latex 4. This material is available free of charge via the Internet at http://pubs.acs.org.

References and Notes

(1) Lee, D. I. Nanostructured latexes made by a sequential multistage emulsion polymerization. *J. Polym. Sci., Part A: Polym. Chem.* **2006**, *44*, 2826–2836.

(2) Sundberg, D. C.; Durant, Y. G. Latex particle morphology, fundamental aspects: A review. *Polym. React. Eng.* **2003**, *11*, 379–432.
(3) Gonzalez-Ortiz, L. J.; Asua, J. M. Development of Particle Morphology in Emulsion Polymerization 1. Cluster Dynamics. *Macromolecules* **1995**, *28*, 3135–3145.
(4) Gonzalez-Ortiz, L. J.; Asua, J. M. Development of particle morphology in emulsion polymerization 3. Cluster nucleation and dynamics in polymerizing systems. *Macromolecules* **1996**, *29*, 4520–4527.
(5) Gonzalez-Ortiz, L. J.; Asua, J. M. Development of particle morphology in emulsion polymerization 2. Cluster dynamics in reacting systems. *Macromolecules* **1996**, *29*, 383–389.
(6) Min, T. I.; Klein, A.; Elaasser, M. S.; Vanderhoff, J. W. Morphology and Grafting in Polybutylacrylate-Polystyrene Core-Shell Emulsion Polymerization. *J. Polym. Sci., Part A: Polym. Chem.* **1983**, *21*, 2845–2861.
(7) Lee, D. I.; Ishikawa, T. The Formation of Inverted Core-Shell Latexes. *J. Polym. Sci., Part A: Polym. Chem.* **1983**, *21*, 147–154.
(8) Sheu, H. R.; Elaasser, M. S.; Vanderhoff, J. W. Uniform Nonspherical Latex-Particles As Model Interpenetrating Polymer Networks. *J. Polym. Sci., Part A: Polym. Chem.* **1990**, *28*, 653–667.
(9) Okubo, M.; Katsuta, Y.; Matsumoto, T. Rupture of Anomalous Composite-Particles Prepared by Seeded Emulsion Polymerization in Aging Period. *J. Polym. Sci., Part C: Polym. Lett.* **1980**, *18*, 481–486.
(10) Okubo, M.; Nakagawa, T. Formation of Multihollow Structures in Cross-Linked Composite Polymer Particles. *Colloid Polym. Sci.* **1994**, *272*, 530–535.
(11) Sundberg, D. C.; Casassa, A. P.; Pantazopoulos, J.; Muscato, M. R.; Kronberg, B.; Berg, J. Morphology Development of Polymeric Microparticles in Aqueous Dispersions 1. Thermodynamic Considerations. *J. Appl. Polym. Sci.* **1990**, *41*, 1425–1442.
(12) Chen, Y. C.; Dimonie, V. L.; Shaffer, O. L.; Elaasser, M. S. Development of Morphology in Latex-Particles - the Interplay Between Thermodynamic and Kinetic-Parameters. *Polym. Int.* **1993**, *30*, 185–194.
(13) Vandezande, G. A.; Rudin, A. Novel Composite Latex-Particles for Use in Coatings. *J. Coat. Technol.* **1994**, *66*, 99–108.
(14) Jonsson, J. E.; Hassander, H.; Tornell, B. Polymerization Conditions and the Development of A Core-Shell Morphology in PMMA /PS Latex-Particles 1. Influence of Initiator Properties and Mode of Monomer Addition. *Macromolecules* **1994**, *27*, 1932–1937.
(15) Chen, Y. C.; Dimonie, V.; Elaasser, M. S. Role of Surfactant in Composite Latex Particle Morphology. *J. Appl. Polym. Sci.* **1992**, *45*, 487–499.
(16) Lee, C. F. Effects of surfactants on the morphology of composite polymer particles produced by two-stage seeded emulsion polymerization. *J. Polym. Sci., Part A: Polym. Chem.* **2005**, *43*, 2224–2236.
(17) Rajatapiti, P.; Dimonie, V. L.; Elaasser, M. S. In-Situ Synthesis of Pba-Graft-Pmma Copolymers to be Used As Compatibilizing Agents in Pba/Pmma Composite Latex-Particles Via the Macromonomer Method. *J. Macromol. Sci., Pure Appl. Chem.* **1995**, *A32*, 1445–1460.
(18) Herrera, V.; Pirri, R.; Leiza, J. R.; Asua, J. M. Effect of in-situ-produced block copolymer on latex particle morphology. *Macromolecules* **2006**, *39*, 6969–6974.
(19) Herrera, V.; Pirri, R.; Asua, J. M.; Leiza, J. R. Morphology control in polystyrene/poly(methyl methacrylate) composite latex particles. *J. Polym. Sci., Part A: Polym. Chem.* **2007**, *45*, 2484–2493.
(20) Karlsson, O. J.; Stubbs, J. M.; Carrier, R. H.; Sundberg, D. C. Dynamic Modeling of Non-equilibrium Latex Particle Morphology Development During Seeded Emulsion Polymerization. *Polym. React. Eng.* **2003**, *11*, 589–625.
(21) Stubbs, J.; Carrier, R.; Sundberg, D. C. Monte Carlo simulation of emulsion polymerization kinetics and the evolution of latex particle morphology and polymer chain architecture. *Macromol. Theory Simul.* **2008**, *17*, 147–162.
(22) Sundberg, E. J.; Sundberg, D. C. Morphology development for three-component emulsion polymers: theory and experiments. *J. Appl. Polym. Sci.* **1993**, *47*, 1277–1294.
(23) Miller, C. M.; Sudol, E. D.; Silebi, C. A.; Elaasser, M. S. Polymerization of Miniemulsions Prepared from Polystyrene in Styrene Solutions 0.1. Benchmarks and Limits. *Macromolecules* **1995**, *28*, 2754–2764.
(24) Wulkow, M. The simulation of molecular weight distributions in polyreaction kinetics by discrete Galerkin methods. *Macromol. Theory Simul.* **1996**, *5*, 393–416.
(25) Chern, C. S.; Poehlein, G. W. Polymerization in nonuniform latex particles: distribution of free radicals. *J. Polym. Sci., Part A: Polym. Chem.* **1987**, *25*, 617–35.
(26) de la Cal, J. C.; Urzay, R.; Zamora, A.; Forcada, J.; Asua, J. M. Simulation of the latex particle morphology. *J. Polym. Sci., Part A: Polym. Chem.* **1990**, *28*, 1011–31.
(27) Chen, Y. C.; Dimonie, V.; El-Aasser, M. S. Interfacial Phenomena Controlling Particle Morphology of Composite Latexes. *Pure Appl. Chem.* **1992**, *11* (64), 1691–1696.
(28) Hu, W.; Koberstein, J. T.; Lingelser, J. P.; Gallot, Y. Interfacial Tension Reduction in Polystyrene/Poly(dimethylsiloxane) Blends by the Addition of Poly(styrene-b-dimethylsiloxane). *Macromolecules* **1995**, *28*, 5209–14.
(29) Landau, D. P.; Binder, K. *A Guide to Monte Carlo Simulations in Statistical Physics*, 2nd ed.; Cambridge University Press: New York, 2005.
(30) Duda, Y.; Vazquez, F. Modeling of composite latex particle morphology by off-lattice Monte Carlo simulation. *Langmuir* **2005**, *21*, 1096–1102.
(31) Duda, Y.; Vakarin, E.; Alejandre, J. Stability and interfacial properties of confined nonadditive hard-sphere binary mixture. *J. Colloid Interface Sci.* **2003**, *258*, 10–19.